Texture density adaptation can be bidirectional

Hua-Chun Sun McGill Vision Research, Department of Ophthalmology, McGill University, Montreal, QC, Canada

Frederick A. A. Kingdom McGill Vision Research, Department of Ophthalmology, McGill University, Montreal, QC, Canada

Curtis L. Baker, Jr. McGill Vision Research, Department of Ophthalmology, McGill University, Montreal, QC, Canada

Texture density has previously been thought of as a scalar attribute on the assumption that texture density adaptation only reduces, not enhances, perceived density (Durgin & Huk, 1997). This "unidirectional" property of density adaptation is in contradistinction to the finding that simultaneous density contrast (SDC) is "bidirectional"; that is, not only do denser surrounds reduce the perceived density of a lower density region, but sparser surrounds enhance it (Sun, Baker, & Kingdom, 2016). Here we reexamine the directionality of density adaptation using random dot patterns and a two-alternative forced choice task in which observers compare the perceived density of adapted test patches with unadapted match stimuli. In the first experiment, we observed a unidirectional density aftereffect when test and match were presented simultaneously as in previous studies. However, when they were presented sequentially, bidirectionality was obtained. This bidirectional aftereffect remained when the presentation order of test and match was reversed (second experiment). In the third experiment, we used sequential presentation to measure the density aftereffect for a wide range of adaptor densities (0–73 dots/deg^2) and test densities (1.6, 6.4, and 25.6 dots/deg^2). We found bidirectionality for all combinations of adaptor and test densities, consistent with our previous SDC results. This evidence supports the idea that there are multiple channels selective to texture density in human vision.

Introduction

Texture density (henceforth, "density") is a visual dimension that carries important information about object surfaces, such as their material properties and the location of their boundaries with adjacent textures. For textures comprising discrete elements, density is defined as the number of elements per unit area (Dakin, Tibber, Greenwood, Kingdom, & Morgan, 2011; Durgin, 1995; Durgin & Huk, 1997; Tibber, Greenwood, & Dakin, 2012). Evidence shows that density is processed separately from other visual dimensions, such as spatial frequency and contrast (Durgin, 1996, 2001; Durgin & Hammer, 2001; Durgin & Huk, 1997; Sun et al., 2016), giving rise to the idea that there are specialized neural channels for coding density (Mackay, 1973; Sun et al., 2016). How exactly density is coded, however, is not presently clear.

Important insights into density coding have come from demonstrations showing that adapting to a given density can alter the perceived density of a subsequently presented test density. These studies have suggested that this "density aftereffect" is unidirectional; i.e., density adaptation only ever reduces, never increases, the perceived density of the test (Durgin, 1995, 1996; Durgin & Huk, 1997; Durgin & Proffit, 1996). Hence, relatively sparse adaptors are deemed to have little adaptive effect (Durgin & Huk, 1997), if anything, reducing rather than increasing the perceived density of the test (Durgin & Proffit unpublished paper described in Durgin, 1996). The unidirectionality of the density aftereffect suggests that density is encoded as a scalar dimension, akin to contrast, rather than via a set of channels selective to different ranges of density.

Some recent findings, however, have prompted us to reexamine here the directionality of the density aftereffect. One of these is our investigation of simultaneous density contrast (SDC), a phenomenon first reported by Mackay (1973), in which the perceived density of a textured region is altered by a surround of different density (Sun et al., 2016). Through systematic manipulation of surround densities, from very sparse to very dense, we found that the

Citation: Sun, H.-C., Kingdom, F. A. A., & Baker, C. L., Jr. (2017). Texture density adaptation can be bidirectional. *Journal of Vision, 17*(8):9, 1–10, doi:10.1167/17.8.9.

doi: 10.1167/17.8.9 Received January 20, 2017; published July 18, 2017 ISSN 1534-7362

perceived density of the center area is shifted from more to less dense than the surround—in other words, we found that SDC is bidirectional. Other dimensions that show bidirectional simultaneous contrast effects, such as orientation (Blakemore, Carpenter, & Georgeson, 1970; Clifford, 2014) and spatial frequency (Klein, Stromeyer, & Ganz, 1974), typically also show bidirectional aftereffects (Blakemore et al., 1970; Klein et al., 1974). This begs the question: why not also density? The other reason for wanting to reexamine the directionality of the density aftereffect is the recent finding that the numerosity aftereffect, in which the perceived numerosity of a dot pattern is altered following adaptation to a dot pattern with a different numerosity (Burr, Anobile, & Turi, 2011; Burr & Ross, 2008), is, at least in relatively sparse patterns, bidirectional (Arrighi, Togoli, & Burr, 2014; Burr & Ross, 2008). Because for a given stimulus area density and numerosity are necessarily confounded, it would seem likely that the density aftereffect might too be bidirectional.

In the experiments described below, we reexamine the density aftereffect. In Experiment 1, the size of the density aftereffect is compared between two ways of presenting the test and match stimuli: simultaneously and sequentially (test first, then match). We tested the two presentation orders because previous studies of the density aftereffect using simultaneous presentation found it to be unidirectional (Durgin, 1995, 1996; Durgin & Huk, 1997; Durgin & Proffit, 1996), whereas studies of the numerosity aftereffect using sequential presentation found it to be bidirectional (Arrighi et al., 2014; Burr & Ross, 2008). In Experiment 2, we measured the effect of reversing the test–match sequential order. In the main experiment, we measured the density aftereffect across a range of adaptor and test densities in order to determine the pattern of its directionality. We demonstrate that measurements of the density aftereffect can show either unidirectional or bidirectional effects, dependent upon how the test and match are presented. For sequential presentation, we demonstrate bidirectional adaptation across a wide range of densities.

General methods

Subjects

Two of the authors (HCS and FK) and two naive volunteers (AF and YSW) participated in Experiments 1 and 3. HCS and AF also participated in Experiment 2. All had normal or corrected-to-normal vision.

Apparatus

Stimuli were generated using the Psychophysics Toolbox (Brainard, 1997; Kleiner, Brainard, & Pelli, 2007; Pelli, 1997) with custom code in Matlab and presented on a CRT monitor (Sony Trintron GDM-F520, 20-in., 1600 × 1200 pixels, 85 Hz). Screen luminance was measured with an Optikon universal photometer and linearized using Mcalibrator2 (Ban & Yamamoto, 2013). Viewing distance was 57 cm.

Stimuli

Stimuli consisted of quasirandomly placed "dots," each a uniform disc of diameter 0.12 deg rendered with Psychophysics Toolbox's "DrawDots" function. The minimum interdot distance was set to be inversely proportional to dot density, using the formula $1.68 \times (\text{density} \times 0.167)^{-0.5}$. This spacing restriction not only prevented overlap of dots, but also eliminated the occurrence of dot clusters interspersed with blank areas in relatively sparse displays; in other words, it produced a relatively uniform textural coverage, holding constant what Durgin (1995) has referred to as the "ratio of regularity."

Three kinds of stimuli were presented within each block of trials: adaptor, match, and test. For the test and match stimuli, half of the dots were black (7 cd/m^2), and the remainder white (115 cd/m^2), all placed on a midgray background (61 cd/m^2), giving a Michaelson contrast of 88.5%. The adaptors were similarly constructed, but their Michaelson contrast was reduced to 44.25% to minimize contrast adaptation effects. Each dot texture pattern was presented within a circular area 4.35 deg in diameter, which was centered 3.45 deg away from fixation. The adaptors and test were presented at the same position, either top left or bottom right with respect to the fixation target. The match was presented correspondingly either bottom left or top right (Burr & Ross, 2008).

The test stimulus was fixed at a specified density, and a set of match stimuli was generated and stored prior to the experiments, ranging across 165 logarithmically spaced density levels, from very sparse (0.13 dots/deg^2) to very dense (73.0 dots/deg^2). The match stimulus for each trial was selected from the 165 levels based on a staircase procedure. All the above aspects of stimulus parameters are the same for all three experiments.

Procedure

At the beginning of each block of trials, there was a 30-s initial adaptation period with a beep at 27 s to alert observers to the first trial. During the adaptation

period, adapting stimuli were presented 30 times, each for 600 ms, separated by 400-ms blank periods (Figure 1). Then a test and a match were shown for 600 ms, either sequentially (Figure 1A) with the two stimuli separated by a 400-ms interstimulus interval (ISI) or simultaneously (Figure 1B). Observers pressed buttons on a numeric keypad to indicate which stimulus appeared to be more dense. No feedback was provided. There was a 7-s top-up adaptation between subsequent test–match presentations within the trial block. Observers were allowed to make a response at any time during the top-up period. Missed trials, never more than three in a 120-trial set, were not included in either the staircase procedure or the subsequent fitting of psychometric functions (PFs); see below. If the observer did not respond in a trial, the next trial would remain the same match density; i.e., the same trial was repeated except that the dot positions of adaptor/test/match were randomly rechosen. A fixation cross (0.34 deg in width) was always presented in the center of the screen, and observers were required to fixate throughout the experiment to avoid misalignment of the retinal images of adaptor and test areas. The fixation cross changed from black to white when the test and match were presented in order to help distinguish them from the adaptors. The positions of the adaptors/test (either at top left or bottom right) and match (bottom left when adaptor/test was top left, top right when the adaptor/test was bottom right) were fixed within a block and switched between blocks in order to avoid residual aftereffects from the previous block. The positions of test and match were therefore balanced in both left–right and top–bottom positions.

During a given block of trials, the test density was fixed while the match density was adjusted using a one-up, one-down staircase procedure (Kingdom & Prins, 2016). The match density for the first trial was randomly chosen in the range bracketing 6–10 levels above or below the physical density of the test. In Experiments 1 and 2, the match density change for the next 11 trials was gradually reduced from 12 to two levels and then remained constant for the remaining 18 trials (30 trials in total). In Experiment 3, match density changes were scaled in proportion to the test densities (see Experiment 3).

Data analysis was the same as in Sun et al. (2016). Responses were first summed across the four staircases that were run for each condition (see below). The match and test density levels were then log-transformed because they were logarithmically spaced. A logistic function was then fit to each PF using the Palamedes Toolbox (Prins & Kingdom, 2009) with a maximum likelihood criterion. Points of subjective equality (PSEs) were estimated from the fits, which were then transformed back to linear scale values. To estimate standard errors for PSEs, we performed a bootstrap analysis (Efron & Tibshirani, 1994) in Palamedes based on 400 resamplings per PF (Kingdom & Prins, 2016).

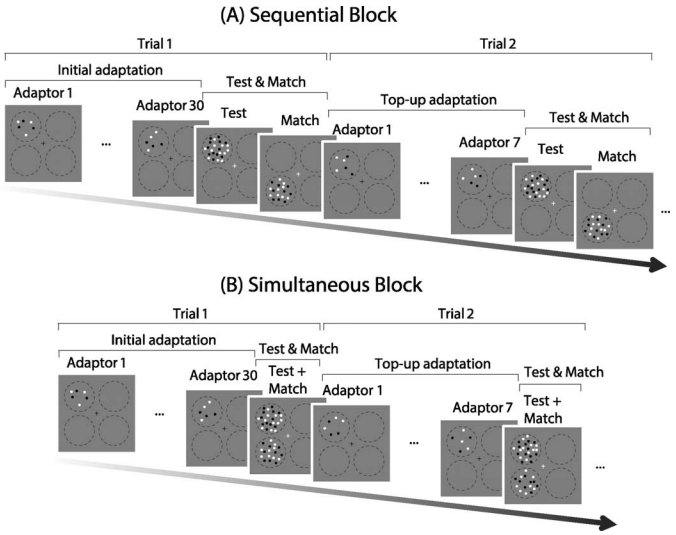

Figure 1. The stimulus presentation protocol for the initial adaptation period and first test–match presentations in a trial block, for (A) sequential and (B) simultaneous presentations of test and match stimuli. A 30-s initial adaptation period was presented in the beginning and then reduced to 7-s top-up adaptations for subsequent trials. Note that all stimuli were presented for 600 ms followed by a 400-ms ISI (not shown in the figure panels). In the sequential condition (A), test and match were presented in two intervals, and in the simultaneous condition (B), the two were presented in the same interval. In this example of a trial block, all stimuli were presented on the left side (adaptors/test: top left; match: bottom left) of the fixation target. In the other half of the trial blocks, all stimuli were presented on the right side with adaptors and tests at bottom right and match at top right. The dashed circles indicating the four possible stimulus locations were not visible in the actual experiment. Note that this schematic depiction is for demonstration purposes, and the actual size and scale of stimuli are as described in Stimuli.

Experiment 1

In pilot experiments, it appeared that the directionality of the density adaptation aftereffect depended on whether the test and match were presented simultaneously or in sequential temporal intervals. The aim of this first experiment was to formally test this relationship. Although sequential presentation is rarely used in aftereffect studies, it is the method that revealed bidirectionality in the numerosity aftereffect (Arrighi et al., 2014; Burr & Ross, 2008).

We evaluated three adaptor densities, 0, 0.74, and 33.7 dots/deg^2, with a test density of 6.6 dots/deg^2. Each participant completed four sessions (two sequen-

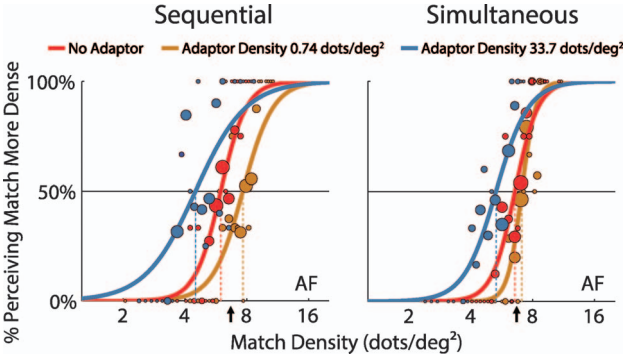

Figure 2. Psychometric functions for naive observer AF for sequential (left) and simultaneous (right) presentations of test and match stimuli. Each graph plots the percentage of times the match appears to be more dense than the test as a function of match density. Test density is 6.6 dots/deg^2 as indicated by the arrow. Adaptor densities are 0 (red), 0.74 (brown), and 33.7 dots/deg^2 (blue). The diameters of filled circles correspond to the number of trials tested with that value of match density as determined by the staircase procedure. Continuous lines are best-fitting logistic functions. The estimated PSEs are the match density values at which the logistic curve-fits intersect the 50% horizontal line.

tial and two simultaneous in a randomized order), each having six blocks (= six staircases, 30 trials each) with the three adaptor conditions each presented twice. Thus, in total, there were four staircases (2 blocks × 2 sessions) for each condition, resulting in 120 trials per condition. In the sequential sessions, the test was followed by a match (each for 600 ms) separated by an ISI of 400 ms as shown in Figure 1A. In the simultaneous sessions, the test and match were presented at the same time (Figure 1B).

Example PFs for naive observer AF are shown in Figure 2 for adaptor densities of 0 (red), 0.74 (brown), and 33.7 dots/deg^2 (blue) with results for sequential and simultaneous presentations in the left and right panels, respectively. Each PF shows the percentage of trials in which the match appeared to be more dense than the test as a function of the match density. The fitted PSEs are shown as the vertical dashed lines. The size of each data point indicates the relative number of trials at each match density. Due to the nature of the staircase procedure, the trials tend to be concentrated around the PSE. In sequential sessions, the PF for the sparser adaptor (brown) is shifted to the right and the PF for denser adaptor (blue) is shifted to the left of the "no adaptor" PF (red), demonstrating a pronounced bidirectional density aftereffect. In the simultaneous sessions (right graph in Figure 2), there is a similar shift of the denser adaptor PF (blue), but there is hardly any shift of the sparser adaptor PF (brown); thus, for simultaneous presentations, the aftereffect is more or less unidirectional.

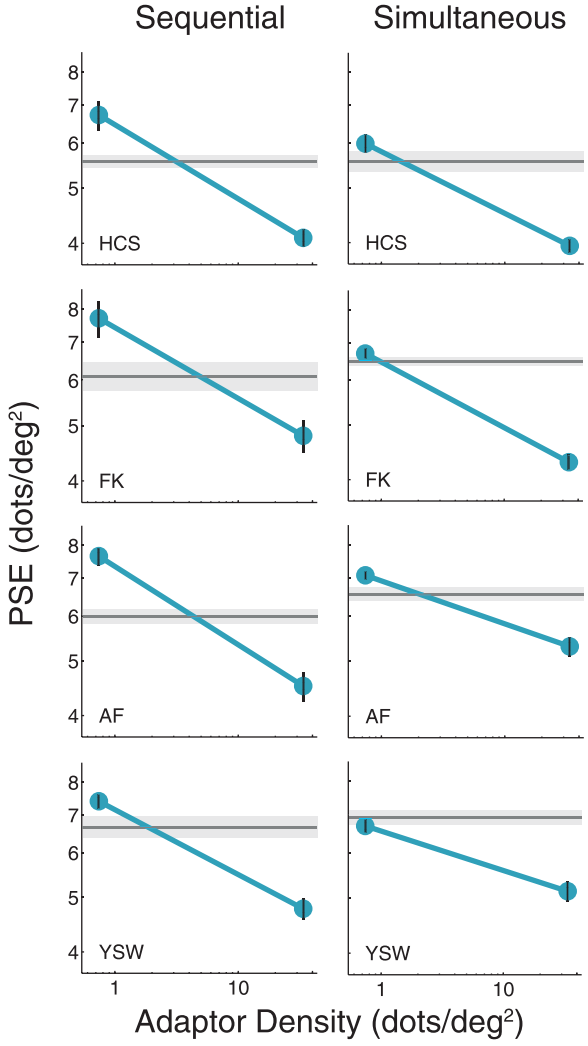

Figure 3. Individual observers' PSE results from Experiment 1. Graphs show individual PSE data as a function of adaptor density for the four observers. Left panels show PSE values for sessions with sequential presentations and right for simultaneous sessions. Each row shows results for one observer. Adaptor densities were 0.74 and 33.7 dots/deg^2, and test density was 6.6. dots/deg^2. No-adaptation PSEs are indicated by the horizontal gray lines. Error bars (light gray areas for no-adaptation conditions) are bootstrap-estimated standard errors.

The PSEs for the four observers are shown in Figure 3. Each graph shows PSE as a function of adaptor density with sequential and simultaneous sessions in the left and right panels for comparison. No-adaptation PSEs are indicated by the horizontal gray lines. Points above the gray lines imply that the test density appeared to be more dense, and points below the gray lines imply that the test density appeared to be less dense compared to the no-adaptation baselines. In sequential sessions (Figure 3, left column), the patterns of the data are generally consistent across observers in showing a bidirectional effect of density adaptation with quite large PSE shifts below and above baseline.

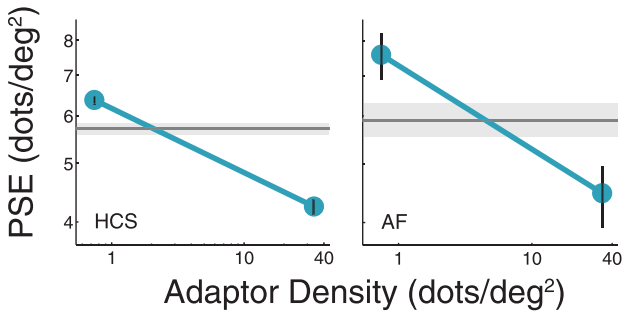

Figure 4. Individual observers' PSE results for Experiment 2. Graphs show individual PSE data as a function of adaptor density for observers HCS and AF. Sequential presentations are used, but unlike in Experiment 1, the match is always presented first, followed by the test. Other experimental conditions were the same as in Experiment 1.

For the sparser adaptor condition, the shifts of perceived density are on average 21.5% across the four observers, and the shifts for the denser adaptor condition are in the opposite direction, on average about 25.2%. The magnitude of density aftereffect is similar to the magnitude of SDC we reported previously (Sun et al., 2016). This demonstrates that under sequential presentation the density aftereffect is bidirectional. However when the test and match were presented simultaneously (Figure 3, right column), the results for all four observers showed a unidirectional adaptation effect with quite large PSE shifts below baseline for the high adaptor density (26.9% on average) but little or no change for the sparser adaptor (3.9% on average). Possible reasons for the sequential versus simultaneous differences are discussed later.

Experiment 2

In the sequential conditions of the previous experiment, test and match were shown in a fixed order with the test first, immediately following adaptation, to potentially maximize the aftereffect. It is possible that the bidirectional result observed in sequential presentation might have been a consequence of this choice of order (e.g., greater attention in the adapted region when the test was presented immediately after, adaptation of the match by the test, etc.). To test this possibility, we reversed the order, presenting the match before the test. All the procedures were otherwise the same as in the sequential conditions of Experiment 1 except that the presentation times of test and match were swapped.

The PSEs for the two observers (HCS and AF) are shown in Figure 4. Each graph shows PSE as a function of the adaptor density (0, 0.74, and 33.7 dots/deg^2) with test density 6.6 dots/deg^2. Similar to Experiment 1 (Figure 3 left panels, HCS and AF), the results again show a bidirectional effect of density adaptation. This evidence demonstrates that the bidirectionality observed in Experiment 1 is not due to the particular presentation order of test and match. The density aftereffect size, however, is slightly reduced in both directions—presumably this is because the tests were shown with a 1-s greater delay following the adaptation. We therefore used test-first sequential presentation in the main experiment below.

Experiment 3

In this experiment, we use test-first sequential presentation to assess the patterns of directionality across a wide range of adaptor and test densities (Table 1). Three test density levels were employed: 1.6, 6.4, and 25.6 dots/deg^2. For test density 1.6 dots/deg^2, the adaptor was set to one of eight relative density levels: test density × 0 (no-adaptor baseline), 0.25, 0.5, 1, 2, 4, 8, or 16 (absolute densities of 0, 0.4, 0.8, 1.6, 3.2, 6.4, 12.8, and 25.6 dots/deg^2). For test density 6.4 dots/deg^2, the adaptor density levels were test density × 0, 0.125, 0.25, 0.5, 1, 2, 4, or 8 (absolute densities of 0, 0.8, 1.6, 3.2, 6.4, 12.8, 25.6, and 51.2 dots/deg^2). For the test density 25.6 dots/deg^2 condition, adaptor densities were test density × 0, 0.06, 0.125, 0.25, 0.5, 1, 2, or 2.85 (absolute densities of 0, 1.6, 3.2, 6.4, 12.8, 25.6, 51.2, and 73.0 dots/deg^2). The last condition (73.0 dots/deg^2) was not a proportional increase as for the other density levels to avoid exceeding the maximum possible density

Test density (dots/deg^2)	Relative adaptor density (absolute adaptor density, dots/deg^2)							
1.6	0	0.25	0.5	1	2	4	8	16
	(0)	(0.4)	(0.8)	(1.6)	(3.2)	(6.4)	(12.8)	(25.6)
6.4	0	0.125	0.25	0.5	1	2	4	8
	(0)	(0.8)	(1.6)	(3.2)	(6.4)	(12.8)	(25.6)	(51.2)
25.6	0	0.06	0.125	0.25	0.5	1	2	2.85
	(0)	(1.6)	(3.2)	(6.4)	(12.8)	(25.6)	(51.2)	(73)

Table 1. Test densities and adaptor densities used in Experiment 3. *Notes*: Three test density levels were employed, and adaptor was set to one of eight relative density levels. Absolute adaptor densities are shown in parentheses.

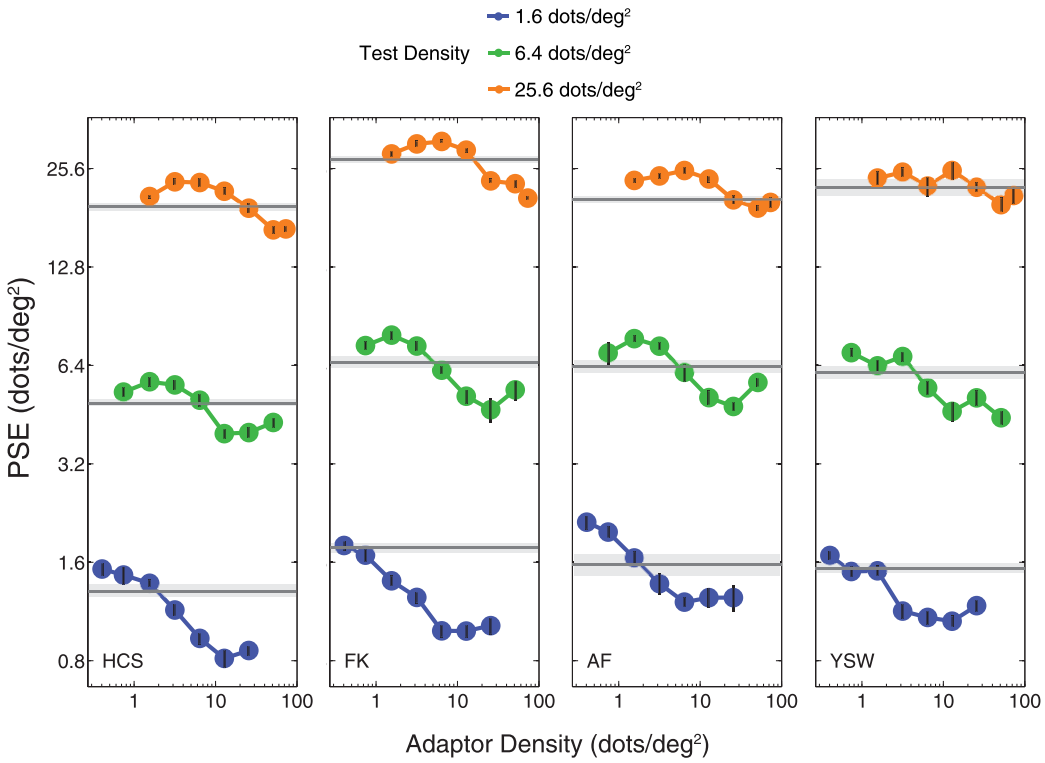

Figure 5. Individual observers' PSE results for Experiment 3. Graphs depict individual PSE values as a function of adaptor density for the four observers, using sequential presentation. Each column shows results for one observer. Blue symbols and lines show PSE values for the 1.6 dots/deg^2, green for 6.4 dots/deg^2, and orange for the 25.6 dots/deg^2 test condition. No-adaptor PSEs are indicated by the horizontal gray lines. Standard error bars are calculated as in Experiment 1.

(to avoid overlapping dots) in our stimulus display. Altogether, this experiment consisted of 3 test densities $\times$ 8 relative adaptor densities = 24 conditions in total.

Each participant completed 96 trial blocks (24 conditions $\times$ 4 repetitions) in a randomized order. The procedure was the same as in the sequential sessions of Experiment 1 except that stimulus duration was increased to 750 ms and ISI reduced to 250 ms with a view to increasing the magnitude of the density aftereffect. Each block contained a 30-trial staircase; therefore, a total of 120 trials were collected for each condition.

The jump sizes in the staircases (increment/decrement of match density) were scaled in proportion to the test densities. For the test density of 1.6 dots/deg^2 condition, the jump size was initially seven density levels, and in subsequent match trials of the staircase, it was reduced by one density level every three trials and was then kept at one for the final 11 trials for convergence. For the test density of 6.4 dots/deg^2, these jump sizes were doubled, and they were doubled again for the test density of 25.6 dots/deg^2 condition. Data analysis was performed as in Experiment 1.

The full set of PSEs for the four observers is shown in Figure 5. Each graph shows PSEs as a function of the absolute density of the adaptors. The blue, green, and orange symbols and lines are for the 1.6, 6.4, and 25.6 dots/deg^2 test conditions, respectively. The horizontal gray lines indicate the PSEs for the no-adaptor baseline conditions. The patterns of the data are generally consistent across the three test conditions and the four observers in showing a bidirectional density aftereffect: PSEs were shifted above baselines when adaptors were sparser than tests and shifted below baselines when adaptors were denser.

Notice in Figure 5 that the curves are progressively shifted to the right (i.e., to higher adaptor densities) as the test density becomes higher. To better compare the PSE shifts across test and adaptor densities, we normalized the PSEs to the no-adaptor baselines to derive a dimensionless measure of aftereffect size:

$$\text{Aftereffect size} = \frac{\text{PSE of each condition} - \text{No adaptor PSE}}{\text{No adaptor PSE}} \times 100\%$$

Aftereffect sizes are plotted as a function of relative adaptor density in Figure 6 with the blue, green, and orange symbols and lines for the 1.6, 6.4, and 25.6 dots/deg^2 test conditions. Vertical dashed lines represent points at which physical densities are equal for test and adaptor. Horizontal dashed lines represent points at which no aftereffect is observed (i.e., having the same PSE as the baseline). Again, positive values indicate an

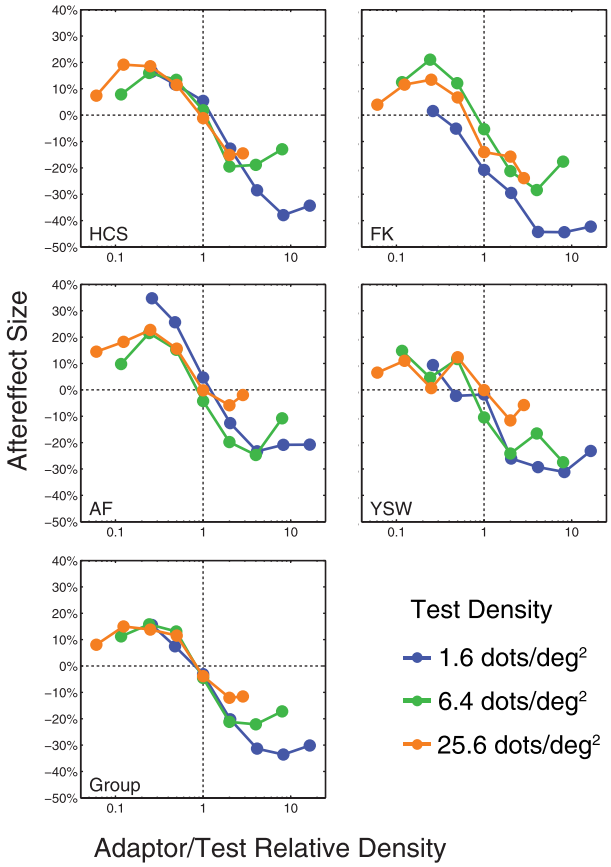

Figure 6. Normalized individual and group aftereffect sizes for Experiment 3. PSE of each condition is subtracted by no-adaptor PSEs, then divided by no-adaptor PSEs, representing percentage of perceived density change compared with no-adaptor baselines. This aftereffect size is plotted as a function of the relative densities of adaptor and test for each of the four observers. Group data (lower left) was the averaged aftereffect size across the four observers. Blue symbols and lines show aftereffect size for the 1.6 dots/deg^2, green for the 6.4 dots/deg^2, and orange for the 25.6 dots/deg^2 test condition. Vertical dashed lines represent points at which adaptor and test densities are physically equal. Horizontal dashed lines represent points at which no aftereffect is observed (i.e., having the same PSE as the no-adaptor baselines). Positive values (above horizontal dashed lines) indicate increased perceived density, and negative values (below horizontal dashed lines) indicate decreased perceived density.

increase in perceived density, and negative values indicating a decrease. The plots illustrate the following features in the data: First, as one would expect, the aftereffect is close to zero when the test and adaptor have the same density. Second, although the positive aftereffects all peak at a relative adaptor density of around 0.25, the peaks of the negative aftereffect shift to higher relative adaptor densities as the test density becomes sparser (about 2, 4, and 8 for test densities 25.6, 6.4, and 1.6 dots/deg^2). Third, the magnitudes of the aftereffect at the peak are similar across test density for the positive aftereffect but increase as the test becomes sparser for the negative aftereffect (12.1%, 22.1%, and 33.6% for test densities 25.6, 6.4, and 1.6 dots/deg^2, respectively). Possible causes for these asymmetrical aftereffect sizes are discussed below.

Discussion

We have found consistent evidence for a bidirectional texture density aftereffect across a 16-fold range of test densities. Adapting to a denser stimulus reduces the perceived density of a subsequently presented test, in line with previous findings (Durgin, 1995; Durgin & Huk, 1997; Durgin & Proffit, 1996). However, we also found that adapting to a sparser density increased perceived test density. This evidence appears to conflict with previous ideas that the density aftereffect is unidirectional and challenges the view that density is coded as a scalar dimension.

Why bidirectionality only with sequential presentation?

In Experiment 1, we found that the density aftereffect was bidirectional when the match and test stimuli were presented sequentially but not simultaneously. The reason for this is as yet unclear, but we can speculate. One possibility is that there are relatively large receptive fields for sparser densities because it is with the sparser density adaptors that simultaneous presentation gives little or no aftereffect. In that case, simultaneously presented match and test stimuli could affect each other via simultaneous density contrast (Sun et al., 2016) or the adaptation could have an effect not only on the test but also on the match stimulus. Either of these possibilities could cause the density aftereffect to become unidirectional.

Numerosity versus density

In some previous studies, observers were asked to judge which of two patterns appeared to contain the greater number of elements (Arrighi et al., 2014; Burr et al., 2011; Burr & Ross, 2008). Demonstrations of the adaptability of this perceived "numerosity" (Arrighi et al., 2014; Burr et al., 2011; Burr & Ross, 2008) as well as findings from single unit neurophysiology (Nieder, 2013, 2016; Ramirez-Cardenas, Moskaleva, & Nieder, 2016; Viswanathan & Nieder, 2013) and human fMRI (Harvey, Klein, Petridou, & Dumoulin, 2013; Santens, Roggeman, Fias, & Verguts, 2010) have supported the

idea that numerosity is a fundamental low-level feature encoded by specific mechanisms. More specifically, measurements of just-noticeable-difference thresholds have suggested that perception of a relatively small number of items is governed by a distinct "numerosity" mechanism or coding scheme (Burr & Ross, 2008), whereas stimuli composed of a multitude of items are represented as "density" (Anobile, Cicchini, & Burr, 2014, 2016; Anobile, Turi, Cicchini, & Burr, 2015). Some other studies, however, have shown similar psychophysical effects (e.g., size of dot patches, contrast polarity of elements, attentional load) for both numerosity and density discrimination, suggesting a common basis for coding density and numerosity (Dakin et al., 2011; Morgan, Raphael, Tibber, & Dakin, 2014; Raphael & Morgan, 2015; Tibber et al., 2012).

Our findings are consistent with the bidirectionality revealed in previous studies measuring the numerosity aftereffect in relatively sparse displays (Burr & Ross, 2008) and with serially presented element arrays (Arrighi et al., 2014). When the stimulus areas of two textures being compared are the same, as in the above studies as well as this one, relative perceived numerosity and relative perceived density are necessarily confounded. Our study, therefore, extends the finding of bidirectionality across a range of test densities, albeit when density is the feature that observers are asked to judge. The test stimulus in Burr and Ross (2008) was set to 50 dots, and adaptors of 12–400 dots (relative numerosity 0.24–8) were tested. In our study, the test stimuli were 23, 95, and 380 dots and adaptors were 6–1,083 dots (relative densities 0.06–16). Our finding of a similar pattern of results across a large range of test and adaptor densities is consistent with a common mechanism across density, but this leaves open the question as to whether the observers' judgments in our study are based on numerosity or density. According to some previous studies measuring discrimination thresholds, numerosity coding switches to density coding at around 2 dots/deg^2 in central vision, reducing to about 1 dot/deg^2 at 6 deg eccentricity (Anobile et al., 2015; Anobile et al., 2016). In our display, the stimulus eccentricity was 3.45 deg, and therefore, according to the dual-regime idea, the switching point should be between 1 and 2 dots/deg^2. In our main experiment, the test densities ranged from a value within the purported numerosity regime (1.6 dots/deg^2) to two densities within the purported density regime (6.4 and 25.6 dots/deg^2). Adaptor densities also ranged across both regimes (0.4–1.6 dots/deg^2). Therefore the most parsimonious account of our results is that a single, density-based mechanism mediates density adaptation, consistent with our previous findings with simultaneous density contrast (Sun et al., 2016) and with other recent work suggesting a shared neural mechanism for coding density and numerosity (Dakin et al., 2011; Morgan et al., 2014; Raphael & Morgan, 2015; Tibber et al., 2012).

Although we argue that our results across different test densities are consistent with a single mechanism, there were some differences in the aftereffect measured for different test densities. Specifically, we found different peak magnitudes of aftereffect and different relative adaptor densities at those peak magnitudes for the three test density conditions when the adaptors were denser than the tests (Figure 6). The reasons for these differences remain unclear, but they may be due to a compression in the internal representation of density as density increases, particularly as density approaches its physical upper limit. If the adaptor and test densities both fall into the more compressed part of the range, they will have more similar internal representations, and as a result, the effects of adaptation will inevitably be less.

Effects of spatial frequency or luminance contrast?

Could spatial frequency adaptation cause the aftereffects that we observe? Previous studies have shown that adapting to textures composed of low as well as high spatial frequency Gabor micropatterns reduces, never enhances, perceived density (Durgin & Huk, 1997) unlike the bidirectional effect of density adaptation revealed here. Moreover, a spatial frequency analysis of our random dot texture stimuli shows that a change in density is not accompanied by a change in relative spatial frequency content (Sun et al., 2016). Thus, it seems unlikely that spatial frequency adaptation could account for our density aftereffects.

Luminance contrast adaptation is also an unlikely cause because contrast adaptation is unidirectional (Georgeson, 1985; Määttänen & Koenderink, 1991). In addition, a previous study using dynamic adaptation indicated that the density aftereffect showed interocular transfer and the contrast aftereffect did not (Durgin, 2001). Also, the density aftereffect cannot be induced by dynamic contrast adaptation (Durgin & Hammer, 2001). Our previous study also showed that SDC is separable from contrast induction (Sun et al., 2016).

Individual differences

Observer YSW exhibits a less pronounced bidirectionality than the other observers due to a relatively weak sparser adaptor aftereffect. However, there is at least one sparser adaptor condition in YSW's data that has a significantly higher PSE than baseline (see the nonoverlapping error bars in Figure 5) for each test

density. In addition, the nine aftereffect values for the sparser adaptors in Figure 6 (left of the vertical dashed line) are together significantly higher than 0, $t(8) = 4.01$, $p < 0.01$. Therefore, we can say that the sparser adaptors did increase perceived density for the results of YSW in general, resulting in a bidirectional aftereffect.

Observer FK also has a relatively weak sparser adaptor aftereffect for the 1.6 dots/deg^2 test condition (blue lines in Figure 5). However, when the data from the first 20 trials of each staircase were selected to fit the psychometric functions for that observer, the positive aftereffect was stronger (and the aftereffects in other conditions remained almost the same). It is possible that with this condition the aftereffect was wearing off after 20 trials.

Conclusion

In three experiments, we found that density adaptation is bidirectional when the test and match stimuli are presented sequentially. The unidirectional density adaptation reported in previous studies might have been due to effects arising from simultaneous presentation of test and match stimuli. Our evidence again supports the idea that there are density-selective channels in the visual system in line with our previous finding in SDC.

Keywords: adaptation, aftereffect, texture, texture density

Acknowledgments

This project was supported by an NSERC (OPG0001978) grant to CB and an NSERC (RGPIN-2016-03915) grant to FK.

Commercial relationships: none.
Corresponding author: Frederick A. A. Kingdom.
Email address: fred.kingdom@mcgill.ca.
Address: McGill Vision Research, Department of Ophthalmology, McGill University, Montreal, QC, Canada.

References

Anobile, G., Cicchini, G. M., & Burr, D. C. (2014). Separate mechanisms for perception of numerosity and density. *Psychological Science*, *25*(1), 265–270, doi:10.1177/0956797613501520.

Anobile, G., Cicchini, G. M., & Burr, D. C. (2016). Number as a primary perceptual attribute: A review. *Perception*, *45*(1–2), 5–31, doi:10.1177/0301006615602599.

Anobile, G., Turi, M., Cicchini, G. M., & Burr, D. C. (2015). Mechanisms for perception of numerosity or texture-density are governed by crowding-like effects. *Journal of Vision*, *15*(5):4, 1–12, doi:10.1167/15.5.4. [PubMed] [Article]

Arrighi, R., Togoli, I., & Burr, D. C. (2014). A generalized sense of number. *Proceedings of the Royal Society of London B: Biological Sciences*, *281*(1797), 1–7, doi:10.1098/rspb.2014.1791.

Ban, H., & Yamamoto, H. (2013). A non–device-specific approach to display characterization based on linear, nonlinear, and hybrid search algorithms. *Journal of Vision*, *13*(6):20, 1–26, doi:10.1167/13.6.20. [PubMed] [Article]

Blakemore, C., Carpenter, R. H. S., & Georgeson, M. A. (1970, Oct 3). Lateral inhibition between orientation detectors in the human visual system. *Nature*, *228*(5266), 37–39, doi:10.1038/228037a0.

Brainard, D. H. (1997). The Psychophysics Toolbox. *Spatial Vision*, *10*(4), 433–436, doi:10.1163/156856897X00357.

Burr, D., Anobile, G., & Turi, M. (2011). Adaptation affects both high and low (subitized) numbers under conditions of high attentional load. *Seeing and Perceiving*, *24*(2), 141–150, doi:10.1163/187847511X570097.

Burr, D., & Ross, J. (2008). A visual sense of number. *Current Biology*, *18*(6), 425–428, doi:10.1016/j.cub.2008.02.052.

Clifford, C. W. G. (2014). The tilt illusion: Phenomenology and functional implications. *Vision Research*, *104*, 3–11, doi:10.1016/j.visres.2014.06.009.

Dakin, S. C., Tibber, M., Greenwood, J. A., Kingdom, F. A. A., & Morgan, M. J. (2011). A common perceptual metric for human discrimination of number and density. *Proceedings of the National Academy of Sciences, USA*, *108*(49), 19552–19557, doi:10.1073/pnas.1113195108.

Durgin, F. H. (1995). Texture density adaptation and the perceived numerosity and distribution of texture. *Journal of Experimental Psychology: Human Perception and Performance*, *21*(1), 149–169, doi:10.1037/0096-1523.21.1.149.

Durgin, F. H. (1996). Visual aftereffect of texture density contingent on color of frame. *Perception & Psychophysics*, *58*(2), 207–223, doi:10.3758/bf03211876.

Durgin, F. H. (2001). Texture contrast aftereffects are

monocular; texture density aftereffects are binocular. *Vision Research*, *41*(20), 2619–2630, doi:10.1016/S0042-6989(01)00121-3.

Durgin, F. H., & Hammer, J. T. (2001). Visual aftereffects of sequential perception: Dynamic adaptation to changes in texture density and contrast. *Vision Research*, *41*(20), 2607–2617, doi:10.1016/S0042-6989(01)00120-1.

Durgin, F. H., & Huk, A. C. (1997). Texture density aftereffects in the perception of artificial and natural textures. *Vision Research*, *37*(23), 3273–3282, doi:10.1016/S0042-6989(97)00126-0.

Durgin, F. H., & Proffit, D. R. (1996). Visual learning in the perception of texture: Simple and contingent aftereffects of texture density. *Spatial Vision*, *9*(4), 423–474, doi:10.1163/156856896X00204.

Efron, B., & Tibshirani, R. J. (1994). *An introduction to the bootstrap*. Boca Raton, FL: CRC Press.

Georgeson, M. A. (1985). The effect of spatial adaptation on perceived contrast. *Spatial Vision*, *1*(2), 103–112, doi:10.1163/156856885X00125.

Harvey, B. M., Klein, B. P., Petridou, N., & Dumoulin, S. O. (2013, Sept 6). Topographic representation of numerosity in the human parietal cortex. *Science*, *341*(6150), 1123–1126, doi:10.1126/science.1239052.

Kingdom, F. A. A., & Prins, N. (2016). *Psychophysics: A practical introduction* (2nd ed.). London: Academic Press.

Klein, S., Stromeyer, C. F., & Ganz, L. (1974). The simultaneous spatial frequency shift: A dissociation between the detection and perception of gratings. *Vision Research*, *14*(12), 1421–1432, doi:10.1016/0042-6989(74)90017-0.

Kleiner, M., Brainard, D., & Pelli, D. (2007). What's new in Psychtoolbox-3? *Perception*, *36*(14), 1.

Määttänen, L. M., & Koenderink, J. J. (1991). Contrast adaptation and contrast gain control. *Experimental Brain Research*, *87*(1), 205–212, doi:10.1007/BF00228521.

Mackay, D. M. (1973, Sept 21). Lateral interaction between neural channels sensitive to texture density? *Nature*, *245*(5421), 159–161, doi:10.1038/245159a0.

Morgan, M. J., Raphael, S., Tibber, M. S., & Dakin, S. C. (2014). A texture-processing model of the 'visual sense of number'. *Proceedings of the Royal Society of London B: Biological Sciences*, *281*(1790), 1–9, doi:10.1098/rspb.2014.1137.

Nieder, A. (2013). Coding of abstract quantity by 'number neurons' of the primate brain. *Journal of Comparative Physiology A*, *199*(1), 1–16, doi:10.1007/s00359-012-0763-9.

Nieder, A. (2016). The neuronal code for number. *Nature Reviews Neuroscience*, *17*(6), 366–382, doi:10.1038/nrn.2016.40.

Pelli, D. G. (1997). The VideoToolbox software for visual psychophysics: Transforming numbers into movies. *Spatial Vision*, *10*(4), 437–442, doi:10.1163/156856897X00366.

Prins, N., & Kingdom, F. A. A. (2009). *Palamedes: Matlab routines for analyzing psychophysical data*. Retrieved from http://www.palamedestoolbox.org/

Ramirez-Cardenas, A., Moskaleva, M., & Nieder, A. (2016). Neuronal representation of numerosity zero in the primate parieto-frontal number network. *Current Biology*, *26*(10), 1285–1294, doi:10.1016/j.cub.2016.03.052.

Raphael, S., & Morgan, M. J. (2016). The computation of relative numerosity, size and density. *Vision Research*, *124*, 15–23, doi:10.1016/j.visres.2014.12.022.

Santens, S., Roggeman, C., Fias, W., & Verguts, T. (2010). Number processing pathways in human parietal cortex. *Cerebral Cortex*, *20*(1), 77–88, doi:10.1093/cercor/bhp080.

Sun, H.-C., Baker, J. C. L., & Kingdom, F. A. A. (2016). Simultaneous density contrast is bidirectional. *Journal of Vision*, *16*(14):4, 1–11, doi:10.1167/16.14.4. [PubMed] [Article]

Tibber, M. S., Greenwood, J. A., & Dakin, S. C. (2012). Number and density discrimination rely on a common metric: Similar psychophysical effects of size, contrast, and divided attention. *Journal of Vision*, *12*(6):8, 1–19, doi:10.1167/12.6.8. [PubMed] [Article]

Viswanathan, P., & Nieder, A. (2013). Neuronal correlates of a visual "sense of number" in primate parietal and prefrontal cortices. *Proceedings of the National Academy of Sciences, USA*, *110*(27), 11187–11192, doi:10.1073/pnas.1308141110.